

Influence of External Traveling-Wave Magnetic Field on Trapped Field of an HTS

Bulk Magnet in an HTSLSM

Jianxun Jin¹, Luhai Zheng¹, Wei Xu², Youguang Guo², and Jianguo Zhu²

¹*Center of Applied Superconductivity and Electrical Engineering, University of Electronic Science and Technology of China, Chengdu 611731, China*

²*Faculty of Engineering and Information Technology, University of Technology Sydney, Sydney, NSW 2007, Australia*

Corresponding authors: Wei Xu, Jianxun Jin

E-mail address: a) weixuinuts@gmail.com (W. Xu), b) jxjin@uestc.edu.cn (J.X. Jin)

Tel.: +86-28-61830798; fax: +86-28-61830798.

Add: School of Automation Engineering, University of Electronic Science and Technology of China

2006 Xiyuan Road, Gaoxin Western District, Chengdu, Sichuan, 611731, China

A single-sided high temperature superconducting (HTS) linear synchronous motor (HTSLSM) has been developed with a pulse magnetization system to obtain the motor secondary HTS bulk magnet array with alternating magnetic poles for the motor secondary. In order to identify the trapped field characteristics of the HTS bulk magnet exposed to the external traveling-wave magnetic field generated by the primary of the HTSLSM, a measurement system has been built up and the relevant experiments have been carried out. As results the relationships between the trapped field attenuation of the HTS bulk magnet and the amplitude, frequency and acting direction of the external traveling-wave magnetic field are experimentally obtained to allow the HTSLSM characteristics to be practically verified ~~are obtained~~.

I. INTRODUCTION

A high temperature superconducting (HTS) bulk can trap a higher magnetic field than a permanent magnet (PM), and can be applied in electric motors, magnetic levitation systems and flywheel energy storage systems etc.¹⁻³ In these applications, the HTS bulk magnets are exposed to the AC external magnetic field. It has been previously observed that

the trapped magnetic field of a HTS bulk can be ~~is~~ affected by the applied AC external magnetic field.^{4,5} It is important to verify the trapped field attenuation characteristics of the HTS bulk magnets used in AC external magnetic field conditions.

The traveling-wave magnetic field generated by an HTS linear synchronous motor (HTSLSM) is a type of

time-varying AC magnetic field. In this paper, a measurement system to investigate the trapped magnetic field attenuation characteristics of the HTS bulk magnet exposed to the external traveling-wave magnetic fields has been built up, and the relationships between the trapped field attenuation with the amplitudes, frequencies and the acting directions of the traveling-wave fields are obtained by the designed experiments.

II. THE MODEL OF HTSLSM

The profile of the developed single-sided HTSLSM is shown in Fig. 1. Its primary has a tooth-slot structure with concentrated winding, whereas the secondary is made of 30 YBCO HTS bulk magnets installed in a cryogenic vessel to form 6 magnetic poles with alternating poles N and S along the moving direction, and same poles installed side by side along the transverse direction to reach a suitable width. Table I lists the main dimensions and parameters of the HTSLSM prototype.

To realize alternating magnetic pole magnetization for the secondary HTS bulk magnets array, a split pulse coil magnetization system has been designed as its principle shown in Fig. 2. After having been magnetized of each one magnetic pole, the magnetization direction is changed to obtain the alternating magnetic pole. After one magnetic pole having been magnetized, the secondary module is moved forward with a step length of one pole pitch τ , and then the next HTS bulk row is magnetized in turn with an opposite magnetization direction, consequently the alternating magnetic poles are obtained.

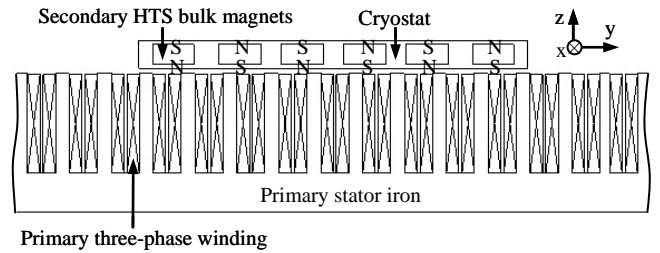


FIG. 1. Profile of the developed HTSLSM.

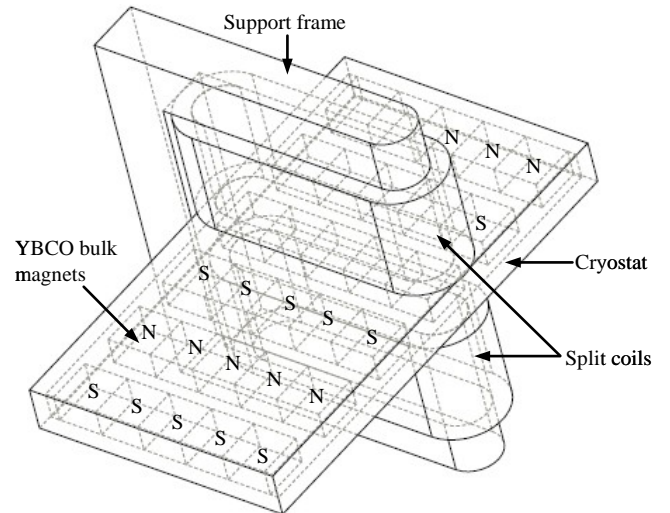


FIG. 2. Scheme of a split pulse coil system for magnetization of the HTS bulk magnet array having alternating magnetic poles.

TABLE I. Dimensions of the single-sided HTSLSM.

Primary	Slot width w_{sl}	20 mm
	Slot depth h_{sl}	100 mm
	Tooth length l_t	10 mm
	Tooth width w_t	150 mm
	Tooth pitch y_1	30 mm
	Pole pitch τ	45 mm
Secondary HTS bulk magnets	Length l_s	30 mm
	Width w_s	30 mm
	Height h_s	15 mm
	Trapped magnetic flux density	0.5 T
	Relative permeability μ_r	0.4
	Number along y direction	6
Number along z direction	5	

The flux linkage distribution along the longitudinal direction of the HTSLSM is shown in Fig. 3. As the figure shown, the majority of magnetic flux flows along the iron core in the primary because of the high permeability and while the flux path is in a regular-like pattern. The relative

permeability of HTS bulk magnet μ_r is set to 0.4 by experience. Considering the reluctances of the HTS bulk magnets and air gaps, the magnetic flux linkage of one coil due to one pole-pair HTS bulk magnets is 0.42 mWb.

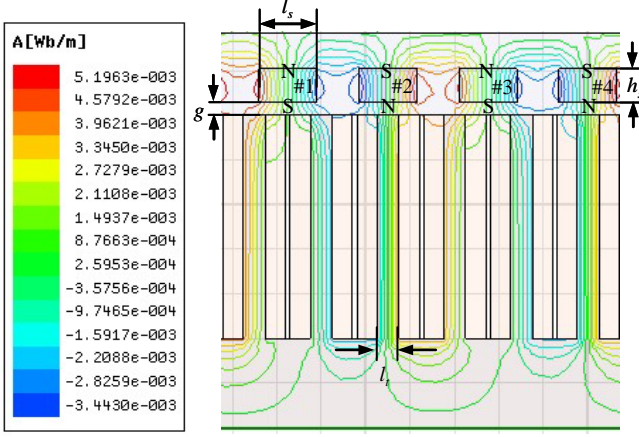


FIG. 3. Flux linkage of the HTSLSM.

III AC LOSS OF HTS BULK EXPOSED TO AC EXTERNAL FIELD

Based on the Bean model, when an HTS bulk is exposed to AC external magnetic field having amplitude B_{ext} parallel to the cylindrical axis (c-axis), the AC loss in the bulk is described as ⁶

$$Q = \begin{cases} \frac{2B_{\text{ext}}^2}{\mu_0} \left(\frac{2\beta}{3} - \frac{\beta^2}{3} \right) & \beta < 1 \\ \frac{2B_{\text{ext}}^2}{\mu_0} \left(\frac{2}{3\beta} - \frac{1}{3\beta^2} \right) & \beta \geq 1 \end{cases} \quad (1)$$

where $\beta = B_{\text{ext}} / B_{\text{em}}$, B_{em} is the full penetration magnetic field equal to $\mu_0 J_c(T) r_0$; $J_c(T)$ the critical current density dependent on bulk temperature T and equal to $J_{c0}(T_c - T)/(T_c - T_0)$; T_c the critical temperature of HTS bulk; T_0 the coolant temperature; J_{c0} the critical current density when $T = T_0$; μ_0 the permeability of vacuum; Q (J/m³/cycle) the loss per cycle per unit volume; and r_0 the radius of HTS bulk.

When the B_{ext} is smaller than 0.1 T, the full penetration magnetic field B_{em} is 0.5 T, the AC loss of HTS bulk versus

B_{ext} is plotted as shown in Fig. 4. As the figure shown, the AC loss exponentially increases with the B_{ext} . When J_{c0} is 2.65×10^7 A/m², T_0 and T_c are 77 K and 91 K respectively, f is 40–5 Hz, r_0 is 0.015 m, the thickness of HTS bulk d is 0.04–0.015 m, the volume of the HTS bulk is $\pi * r_0^2 * d$, then the power loss P ($P(t) = QfV$) of HTS bulk versus T at different B_{ext} is shown in Fig. 5. It can be seen that the power loss increases with T and the amplitude of AC external field. When the B_{ext} is set at a value of 0.05 T, the power loss P versus T for different f is calculated and indicated in Fig. 6. As seen from the figure, P decreases as T and f decrease, and only has a slight difference for various

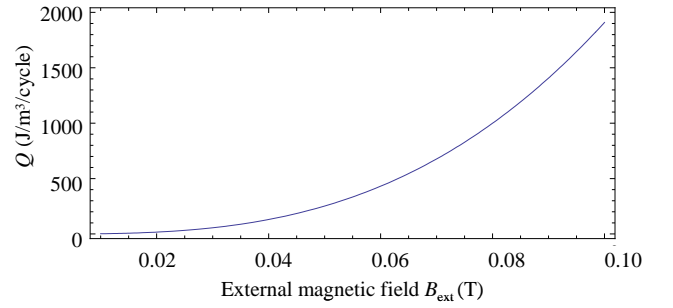


FIG. 4. AC loss of HTS bulk versus external AC magnetic field.

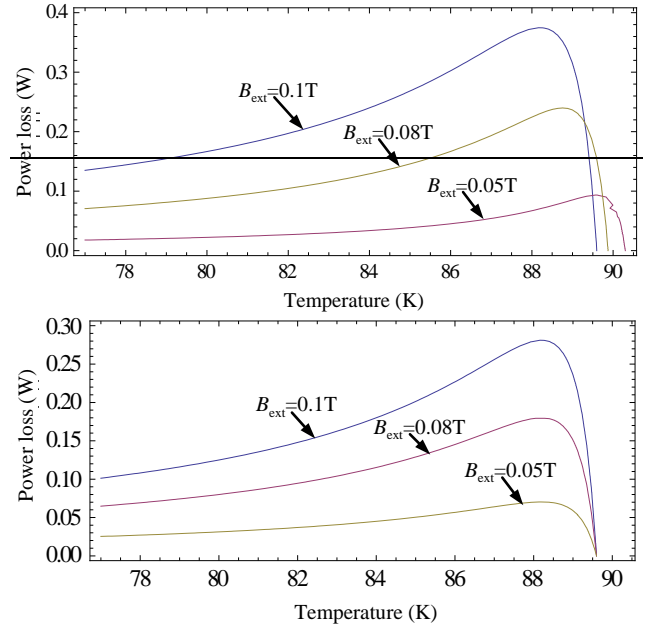


FIG. 5. Power loss versus working temperature T for different B_{ext} .

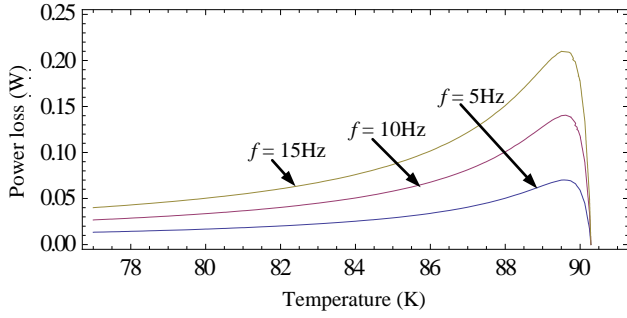


FIG. 6. Power loss versus working temperature T for different f .

When β is more than 1, the external magnetic field completely penetrates into the bulk and the trapped magnetic field disappears when the external field is terminated. Therefore, the maximum trapped magnetic field B_m is

$$B_m(T) = \begin{cases} \mu_0 J_c(T)(r_0 - r_m) & \text{for } \beta < 1 \\ 0 & \text{for } \beta \geq 1 \end{cases} \quad (2)$$

where r_m is the penetration depth of the external magnetic field. As T is increased by the AC loss, then J_c decreases and r_m increases gradually. Thus, B_m could decrease and become zero when β exceeds 1. It can be seen that the attenuation of trapped field is caused by the thermal effect due to AC loss. The larger AC losses in the bulk, the then larger attenuation of the trapped magnetic field could attain.

IV. TESTING SYSTEM

A practical testing system has been built up as shown in Fig. 7. It mainly consists of the YBCO HTS bulk magnets, a linear motor primary stator, a three-phase inverter, a data acquisition system, low temperature Hall sensors, a cryostat and a computer controller. The typical testing procedures are summarized as follows:

1) Obtaining the YBCO HTS bulk magnet by field-cooled (FC) magnetization or pulse magnetization, and then locating it on the long primary stator of linear motor.

2) Applying a three-phase AC current for the primary to generate traveling-wave magnetic field on the surface of primary stator, and then to change changing the frequency and amplitude of the three-phase current to modify the frequency and amplitude of the traveling-wave magnetic field.

3) Measuring the surface magnetic field of YBCO bulk magnet using a Hall matrix at different conditions, and to obtain obtaining the trapped field attenuation characteristics versus different amplitudes and frequencies of the external traveling-wave field.

4) Changing the placement direction of the YBCO bulk magnet, and testing the trapped field attenuation traits at different action directions of the external field.

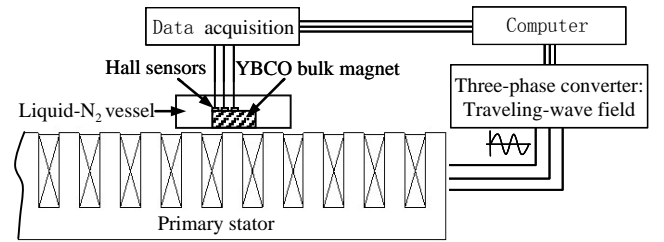


FIG. 6-7. Diagram of the experimental setup.

V. RESULTS AND ANALYSIS

The influence of the external traveling-wave magnetic field amplitude on the trapped field attenuation was investigated experimentally. The trapped field attenuation at the constant frequency of 5 Hz for different armature currents including 2.8 A, 5.45 A, and 10.92 A, was measured as shown in Fig. 8. It shows that the trapped magnetic field attenuation under external traveling-wave magnetic field is apparently different from that of flux creep. When the external traveling-wave magnetic fields are applied, the slope of trapped field attenuation rate increases with the amplitude of traveling-wave fields. It can be seen that the larger amplitude of AC magnetic field, the larger

AC loss [7], resulting in larger trapped field attenuation.

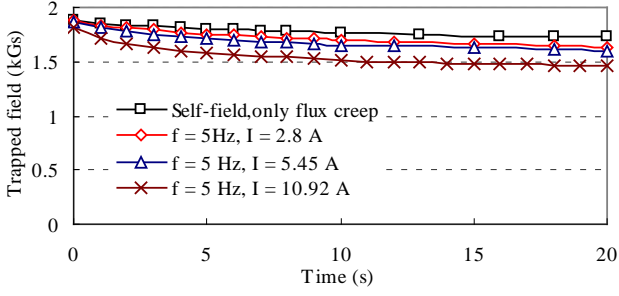


FIG. 7-8. Trapped field influenced by traveling-wave field amplitudes.

The amplitudes of trapped magnetic fields excited by a constant current of 5.45 A, which is achievable for different f , have been measured as shown in Fig. 9. In the figure, the trapped field is almost independent of frequency when f is changed experimentally from 5 to 15 Hz. It means that the eddy-current losses caused by the metal impregnation affect insignificantly the AC loss.

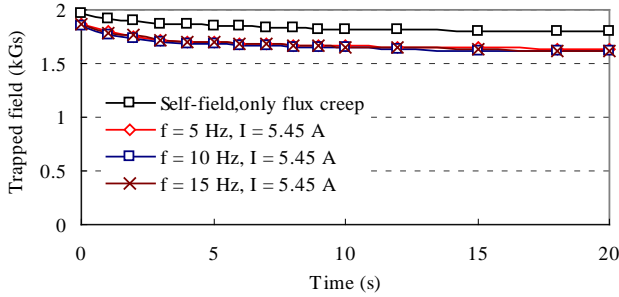


FIG. 9. Trapped field influenced by frequency of traveling-wave field.

The trapped field of the HTS bulk magnet versus different directions of the traveling-wave field is shown in Fig. 9-10. It can be seen that the attenuation of the trapped magnetic field is larger in the case of the perpendicular traveling-wave magnetic field ($c\text{-axis} \perp B_{\text{ext}}$) than that of the parallel ($c\text{-axis} \parallel B_{\text{ext}}$), where the c -axis of the bulk crystal is parallel to the cylindrical HTS bulk axis. It can be explained that when the perpendicular external traveling-wave magnetic field is applied, a shielding current which has a component parallel to the c -axis of the bulk crystal is then induced. The J_c along the c -axis is smaller

than that in the a - b plane where the current holding the trapped field is circulating. Therefore, the AC loss in the bulk caused by the perpendicular traveling-wave magnetic field is larger than that caused by the parallel traveling-wave field, because the parallel AC traveling-wave magnetic field induces the shielding current in the a - b plane of the HTS bulk.⁷

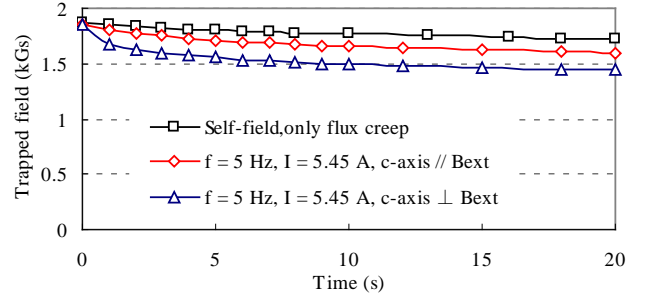


FIG. 9-10. Trapped field influenced by direction of traveling-wave field.

When the HTS bulk magnets are used in the HTSLSM, the cylindrical HTS bulk axis is parallel with the direction of the traveling-wave magnetic field ($c\text{-axis} \parallel B_{\text{ext}}$). The attenuation amplitude of the bulk magnet trapped magnetic field increases approximately linearly with the amplitude of traveling-wave magnetic field increases as illustrated in Fig. 10-11, which was measured five minutes later after applying the external field. The maximum thrust F_{max} versus the current for attenuation and no-attenuation conditions are also shown in Fig. 11. Based on the data measured, the fitting function of the B_{trap} versus exciting current is $B_{\text{trap}} = g_t(0.02x + 1.82)$, where g_t is the time factor related to the interval time to measure. Fitted function of F_{max} versus exciting current for practical attenuation condition is $F_{\text{max}} = G_t(-0.32x^2 + 10.95x - 0.33)$, G_t is the time factor related to the interval time to measure.

From the figure, the F_{max} increase linearly with exciting current at no-attenuation condition theoretically, however,

the slope of F_{\max} decreases with the attenuation amplitude of the trapped field. In order to obtain a required thrust, it is needed to take into account both the exciting current and the trapped field attenuation.

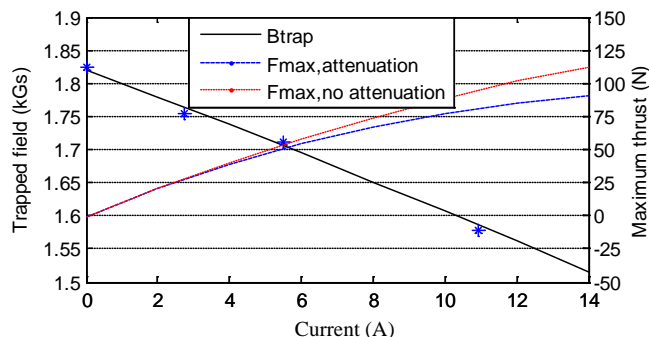


FIG. 10-11. Amplitude of trapped field and $F_{\text{em,max}}$ versus exciting current.

VI. CONCLUSIONS

The trapped field attenuation characteristics of HTS bulk magnet exposed to the external traveling-wave magnetic field generated by the HTSLSM primary have been studied both in theory analysis and measurement. The results show that the trapped magnetic field attenuation is apparently different from that of HTS flux creep, and the attenuation amplitude of the trapped field increases linearly with the amplitude of traveling-wave field. The frequency of traveling-wave field has only a minimal influence on the trapped field attenuation especially at low temperature region, and the attenuation of the trapped field is larger in the case of the perpendicular traveling-wave magnetic field on the cylindrical bulk axis (c-axis) than that of the parallel. The experimental results obtained and the relevant analysis form a base for the HTS bulk magnet array design to suppress the trapped field attenuation in an HTSLSM.

ACKNOWLEDGMENTS

This work has been funded by the Chinese High-Tech R&D (863) Program under Grant No. 2007AA03Z208.

¹S. S. Kalsi, B. B. Gamble, G. Snitchler, and S. O. Ige. in IEEE Power Engineering Society General Meeting, 18(2006).

²J. X. Jin, L. H. Zheng, W. Xu, Y. G. Guo, and J. G. Zhu. J. Appl. Phys. 109, 073916-1(2011).

³M. Strasik, P. E. Johnson, A. C. Day, J. Mittelreider, M. D. Higgins, J. Edwards, J. R. Schindler, K. E. McCrary, C. R. McIver, D. Carlson, J. F. Gonder, and J. R. Hull. IEEE Trans. Appl. Super. 17, 2133(2007).

⁴H. Ueda, M. Itoh, and A. Ishiyama. IEEE Trans. Appl. Super. 13, 2283(2003).

⁵K. Yamagishi, J. Ogawa, O. Tsukamoto, M. Murakami, and M. Tomita. Physica C 392-396, 659(2003).

⁶O. Tsukamoto, K. Yamagishi, J. Ogawa, M. Murakami, M. Tomita. J. Mater. Proc. Technol. 161, 52(2005).

⁷T. Ohyama, H. Shimizu, M. Tsuda, and A. Ishiyama. IEEE Trans. Appl. Super. 11, 1988(2001).

